COMPARISON OF MEASURED AND CALCULATED HYDRAULIC PARAMETERS FOR RECH-1 CHILEAN REACTOR FUEL ELEMENT

CARLOS R. GUTIERREZ ULLOA, CHRISTIAN MARCHANT ASTETE,
Nuclear Materials Department, Chilean Commission of Nuclear Energy (CCHEN)
Amunategui 95, 8340701, Santiago, RM, Chile

EDISON MANRIQUEZ,
Faculty of Physical Sciences and Mathematics, University of Chile
Almirante Beauchef 851, 8370456, Santiago, RM, Chile

ABSTRACT

The Chilean Reactor RECH-1 is a 5-MW pool-type Research Reactor and uses MTR plate type fuel assembly of 3.4gU / cm^3. The design and construction of the reactor was carried out by the CCHEN, Fairey Engineering Limited and the United Kingdom Atomic Authority, and it has been in operation for 43 years.

Nuclear Fuel of RECH-1 has been converted from HEU uranium aluminides to LEU uranium silicide according to international enrichment reduction program.

The Nuclear Fuel Fabrication Facility (NFFF) has established a program to strengthen design capacities in order to develop and validate new designs of Nuclear Fuel Assemblies. To fulfill this objective, an Experimental Loop Test Bench (ELTB) was designed and constructed to determine the hydraulic parameters of Fuel Assemblies (FA) and irradiation devices.

A standard fuel element was introduced in the HLTB and subjected to different flow rates under normal operating conditions.

The dynamic pressure was measured at the input and output of the Fuel Element by the use of pressure transmitters, which allowed the determination of the pressure loss - flow curve.

Followed by simulations to compare measured and calculated hydraulic parameters. The simulations were performed in a CFD software, where the subsets and FA have been simulated for the different fluid velocities.

1. Introduction

The Nuclear Fuel Fabrication Facility (NFFF) supplies Fuel Assemblies (FA) to the Chilean Reactor RECH-1 since 1998 in the framework of the International Enrichment Reduction Program. Nowadays, there is an institutional strengthening program, which proposes to increase capacities in nuclear design, thermos-hydraulic design and mechanical design, with the purpose of designing, manufacturing and supplying FA´s for other Research Reactors abroad.

The general objective of this work is to characterize hydraulically the type flat plates FA of the Research Nuclear Reactor RECH-1.

The specific objectives are: Determine pressure loss curves, under normal operating conditions, by means of numerical simulation. Identify the behavior of the current lines inside the EC in descending way. Corroborate the simulated model by comparison with experimental and analytical data.

To fulfill these objectives, the NFFF has a hydraulic test bench (Hydraulic Loop) designed to simulate the operating conditions of the Research Reactor. Computer and simulation software were supplied by the engineering faculty of the University of Chile. Hydraulic Loop has the capacity to measure the load losses, temperature difference measurement and volumetric flow.

The RECH-1 Reactor is a pool type nuclear research reactor, whose nominal thermal power is 5 [MW]. It uses light water as moderator material and as a cooling material, as an absorbent material uses Cadmium. The main pool has dimensions of 3.05 x 4.95 x 10 [m] depth coated with stainless steel 6 [mm] thick plus 170 cm thick high density concrete. The core is inside the pool [2].

NFFF is a nuclear facility that is part of the Advanced Materials Department (DMA). PEC aims at research and technological development and processing of materials of nuclear interest or use, in particular EC and devices for irradiation of materials in nuclear research reactors.

The fuel assemblies manufactured are of flat plate design with U_3Si_2 uranium silicified meat dispersed in an aluminum matrix, with a density of 3.4 [gU/cm^3]. Device consists mainly of three parts; Filter Box Set (FBS), Fuel Body (FB) and Nozzle (NOZ). In FBS is located at the top of the FA and allows manipulation inside the pool. The NOZ allows accommodating the FA in the core. The FB consists of 16 flat plates, 14 internal plates with a density of 3.4 [gU / cm^3] and 2 external plates with a density of 1.4 [gU / cm^3].

2. Experiment

2.1 Experimental Loop Test Bench (HTLB): A dummy FA was introduced into the HTLB. The bench has a mechanical system, which has the capacity to recirculate a water flow through a hydraulic centrifugal pump with a capacity of up to 50 [m3 / h]. The fluid is stored in a polyethylene pond of 3400[L] [3]. See Figure 1.

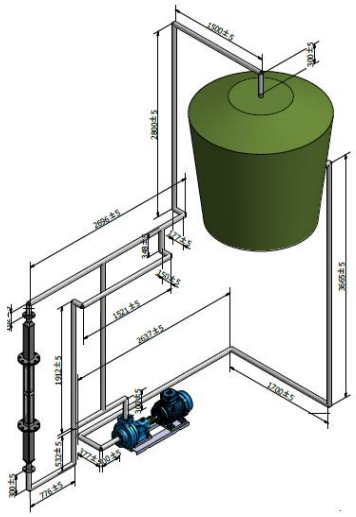

Figure 1: Isometric view of the distribution of components in hydraulic test bench.

2.2 Analytical Calculations: For the analytical calculation of load losses, bibliography was used. (R. Mott, Fluid Mechanics, Mexico: Pearson Education, 2006). A load loss calculation was performed for each case (subset) of the fuel element.

Laminar flow was considered in the FB, moving through two static parallel plates. From the continuity and Navier-Stokes equations, with simplifications of incompressible flow, plane flow and continuity condition; we can express the pressure drop for a horizontal channel as a function of the average speed, as shown in figure 2.

$$\Delta \mathrm{p} = \frac{1{,}2\mu \mathrm{VL}}{a^2}$$

Figure 2: Equation of pressure loss in parallel plates.

The loss coefficient of a perforated plate [4], depends on the porosity of the plate, the edges of the perforations, Reynolds number, and the thickness of the plate. In general, is assumed that the velocity at the center of the contraction is subsonic. The following relationships, shown in Figure 3, are established.

$$k_l = \frac{k_f}{\varphi^2} + \varepsilon k \qquad 30 < R_0 < 10^4 \; to \; 10^5$$

$$k_l = \frac{33/R_0}{\varphi^2} + \varepsilon k \qquad 10 < R_0 < 25$$

$$k_l = \frac{33/R_0}{\varphi^2} \qquad 10 < R_0$$

Figure 3: Pressure loss equations in perforated plates.

The pressure drop in the nozzle is considered as gradual contraction according to the following expression [5], see figure 4:

$$k = \frac{0.8 \cdot sen(\theta/2) \cdot [1 - (D_2/D_1)^2]}{(D_2/D_1)^4} \qquad Si \; \theta \leq 45°$$

$$k = \frac{0.5 \cdot [1 - (D_2/D_1)^2] \cdot \sqrt{sen\,\theta/2}}{(D_2/D_1)^4} \qquad Si \; 45 < \theta \leq 180°$$

Figure 4: Pressure Loss Equations in Nozzles

In the case of cross pieces of the FB, pressure drop is produced by obstacles. See equation in the figure 5 [6].

$$f_{app} = C_{D1}\frac{d}{2L} + C_{D2}\frac{d}{2L}$$

$$h_l = f_{app}\frac{V^2}{2g}$$

Figure 5: Pressure loss equations on crossbars.

2.3 Computational Calculations: CFD has been used for fluid analysis calculations. The system uses the method of finite volumes and moving mesh methods using the governing equations of mass conservation, momentum (Navier-Stokes) and Energy [7]. See figure 6.

$$\nabla \cdot \rho\bar{V} + \frac{\partial \rho}{\partial t} = 0$$

$$-\nabla p + \nabla \cdot \mathrm{T} + \mathrm{f} = \rho\left(\frac{\partial \mathrm{v}}{\partial t} + \mathrm{v} \cdot \nabla \mathrm{v}\right)$$

$$\frac{\partial u}{\partial t} + \nabla \cdot q = 0$$

Figure 6: Equations of mass conservation, momentum (Navier-Stokes) and Energy

The pressure and velocity coupling method SIMPLEC (SIMPLE-Consistent), proposed by Van Doornal and Raithby, has been selected. This model consists of an iterative method where a pressure field is assumed and the Navier-Stokes discretized equations are solved, then the initial pressure field is corrected until a convergence is achieved.

In meshing and quality determination, the ANSYS Fluent software allows the geometry to be approximated by discretization based on points or nodes. These nodes connect to form finite elements that together make up the volume of the material. Each node created on the surface of an object is associated with a differential equation to be solved. In this way, the finer the mesh, the more accurate the solution of the problem.

Two methods, Skewness Method and Aspect Ratio [8] were used to determine the mesh quality. Skeness makes comparison of triangles formed by meshing against equilateral triangles. In the case of Aspect Ratio, measures how tight the control volume is, in triangles and squares is a relationship between the longest side and the shorter side.

3. Results

3.1 Experimental results:

Experimental measurements give the pressure drop for the velocity variation, which are shown in table 1. Two measurements were taken as the frequency of the pump that

handled the system flow varied and shows a third "average" column that is calculated from the two measurements.

	Measurement 1		Measurement 2		Average	
[K Hz]	$[m/s]$	$[Pa]$	$[m/s]$	$[Pa]$	$[m/s]$	$[Pa]$
5	0,0036	800	0,0035	1500	0,0035	1150
10	0,0063	1200	0,0351	1800	0,0207	1500
15	0,1169	1500	0,1198	2600	0,1183	2050
20	0,2045	2400	0,2834	3100	0,2440	2750
25	0,3682	5400	0,4178	4100	0,3930	4750
30	0,5172	7700	0,5259	5200	0,5215	6450
35	0,6545	11400	0,6603	6100	0,6574	8750
40	0,7743	11500	0,7801	7500	0,7772	9500
45	0,8912	12000	0,9204	8100	0,9058	10050
50	1,0197	13100	1,0226	9800	1,0212	11450

Table 1: Experimental results: Pressure drop according to the variation of velocity is obtained through experimental measurements.

3.2 Analytical Results:

Analytical calculations have been carried out to determine the pressure drop of each of the subassemblies, and each value has subsequently been added to obtain the total pressure loss for each speed. The results obtained are shown in Table 2.

	Velocity	Filter Plate	Body	Nozzle	Sum of subsets
#	$[m/s]$	$\Delta P\ [Pa]$	$\Delta P\ [Pa]$	$\Delta P\ [Pa]$	$\Delta P\ [Pa]$
1	0,01	0,3	34,7	0,5	36
2	0,05	8,9	173,6	13,4	196
3	0,1	37,1	347,2	53,6	438
4	0,15	86,6	517,4	118,9	723
5	0,25	258,2	864,6	332,1	1455
6	0,35	508,4	1211,8	652,4	2373
7	0,55	1272,6	1906,3	1614,3	4793
8	0,75	2478,1	2600,7	3004,7	8084
9	0,95	4022,0	3295,1	4823,6	12141
10	1,15	5974,9	3989,6	7071,0	17036

Table 2: Analytical results: Analytical calculations have been performed to determine the pressure loss of each of the subsets

3.3 Computational Results:

The results of the simulations are summarized in Table 3. Is added the "sum" column, which corresponds to the sum of drop pressure of the Filter Box, Body and Nozzle. In addition the column "error" has been added, which is the calculation of the difference between the sum and the results of the whole fuel assemblies.

For the simulations performed in the Filter Box, it has been determined that for a low velocity, the pressure drop is almost null with the increasing tendency as the velocity increases.

In the case of the Fuel Body the pressure drop increases as the speed increases, which is supported by the analytical model discussed above and what physically should occur.

Pressure losses, in the case of the Nozzle, at high velocities, a higher pressure loss jump occurs for a constant velocity change.

Finally, in the case of the complete EC, the simulations were performed for the complete geometry of the fuel element, analysing the results obtained in Table 3, it can be established that from the nominal velocity there is a progressive increase in the pressure drop.

	Fluid			Pressure in subsets				Summation of subsets	
	V	$\dot{m}$	$\dot{Q}$	Filter plate	body	Nozzle	Summation	Fuel Element	Error
#	$[m/s]$	$[kg/s]$	$[m^3/s]$	$\Delta P\ [Pa]$	$\Delta P\ [Pa]$	$\Delta P\ [Pa]$	$\Delta P\ [Pa]$	$\Delta P\ [Pa]$	%
1	0,01	0,058	0,000058	0,75	14,29	2,062	17,1	16,8	2%
2	0,05	0,290	0,00029	10,4	82,8	33,62	126,8	124	2%
3	0,1	0,580	0,00058	38,6	191,2	125,9	355,7	338	5%
4	0,15	0,864	0,0008642	85,2	315,6	262,4	663,2	634	4%
5	0,25	1,444	0,0014442	245	611,8	696,7	1553,5	1465	6%
6	0,35	2,024	0,0020242	439,5	939,8	1317	2696,3	2556	5%
7	0,55	3,184	0,0031842	1805	1390,7	3211	6406,7	5754	10%
8	0,75	4,344	0,0043442	2536	2092,3	5666	10294,3	10106	2%
9	0,95	5,504	0,0055042	3956	2905,7	8833	15694,7	15572	1%
10	1,15	6,664	0,0066642	5118	3182,2	12780	21080,2	22188	5%

Table 3: Analytical results: Summary table of results of loss of load.

Table 4 shows experimental results, analytical results and computational results. In the latter case computational calculations are illustrated in the Integer Element and in Sub-sets.

	Fluid			Computational		Analytical		Experimental Case	
	V	$\dot{m}$	$\dot{Q}$	Subset	Fuel Assembly	Fuel Assembly			
#	$[m/s]$	$[kg/s]$	$[m^3/s]$	$\Delta P\ [Pa]$	$\Delta P\ [Pa]$	$\Delta P\ [Pa]$		$[m/s]$	$\Delta P\ [Pa]$
1	0,01	0,058	0,000058	17	17	36	1	0,0035	1.150
2	0,05	0,290	0,00029	127	124	196	2	0,0207	1.500
3	0,1	0,580	0,00058	356	338	438	3	0,1183	2.050
4	0,15	0,864	0,0008642	663	634	723	4	0,2440	2.750
5	0,25	1,444	0,0014442	1.554	1.465	1.455	5	0,3930	4.750
6	0,35	2,024	0,0020242	2.696	2.556	2.373	6	0,5215	6.450
7	0,55	3,184	0,0031842	6.407	5.754	4.793	7	0,6574	8.750
8	0,75	4,344	0,0043442	10.294	10.106	8.084	8	0,7772	9.500
9	0,95	5,504	0,0055042	15.695	15.572	12.141	9	0,9058	10.050
10	1,15	6,664	0,0066642	21.080	22.188	17.036	10	1,0212	11.450

Table 4: Comparison of computational, analytical and experimental results.

Table 5 shows the percentage of error that exists between the computational results and the experimental results.

Computational			Experimental Case			
#	$[m/s]$	$\Delta P\ [Pa]$	#	$[m/s]$	$\Delta P\ [Pa]$	Error
1	0,01	16,8	1	0,0035	1150	99%
3	0,1	338	3	0,1183	2050	84%
5	0,249	1465	4	0,2440	2750	47%
6	0,349	2556	5	0,3930	4750	46%
7	0,549	5754	6	0,5215	6450	11%
8	0,749	10106	8	0,7772	9500	6%
9	0,949	15572	9	0,9058	10050	55%

Table 5: Computational and experimental comparison.

3.3.1 Graphs: Starting from the values in Table 4, the graph of Figure 7 is generated, showing the drop pressure curve as a function of velocity, using the Analytical Fuel Assemblies measurements, Computational Subset method measurements (sum of the Filter Box , Body and Mouthpiece), Computational fuel assemblies measurements and experimental measurements. In addition, the graph of Figure 8, which compares the drop pressure for each subset, is created.

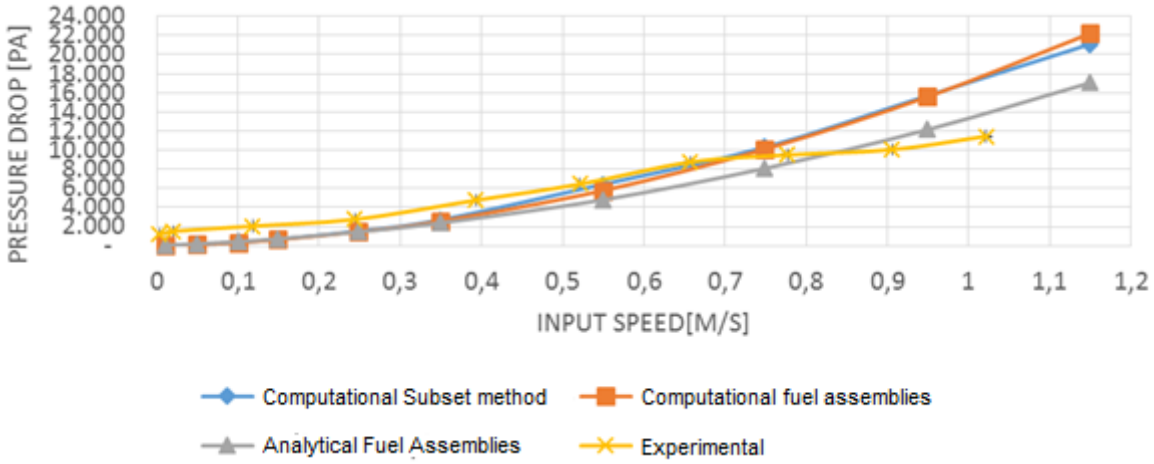

Figure 7: Curve that compares the loss of pressure between experimental, analytical and computational whole and computational summative modes.

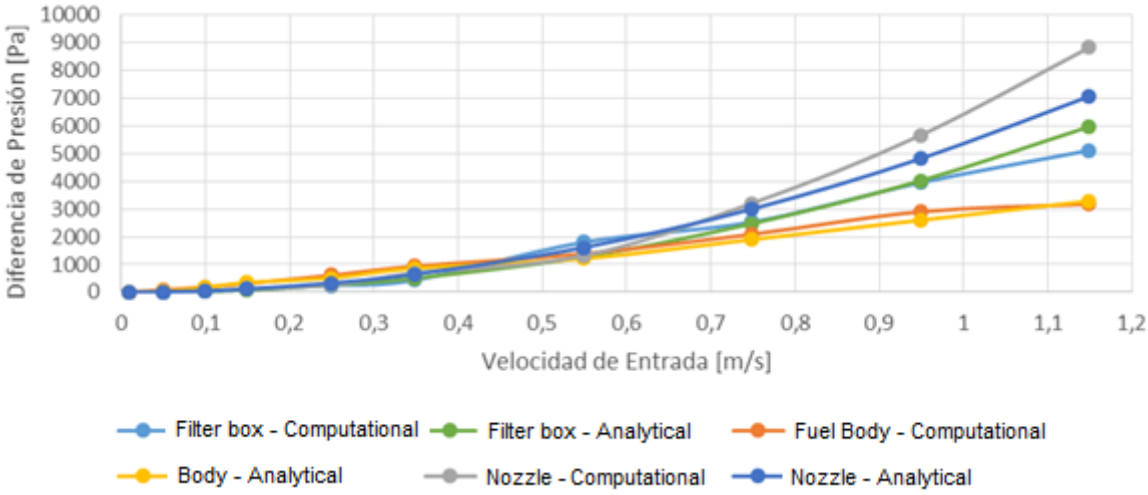

Figure 8: Curve that compares the pressure loss for each subset

3.3.2 Results: Pressure contour diagrams and current lines:

3.3.2.1 Simulations filter box: Figure 9 shows the drop pressure between the inlet and the outlet of the control volume of the filter box. The part that generates the greatest drop pressure is the filter plate, then follow the crossbars; figure 10 shows current lines inside the filter box, it can be seen that flow recirculation is generated in in the areas of the orientation piece and crosspiece, and filter plate, due to a sudden strangulation in the orifices. The computational simulation of each speed required approximately 10 hours of computational calculations, in order for the solution to converge. Which in total translates into 100 hours of computational use to obtain the results.

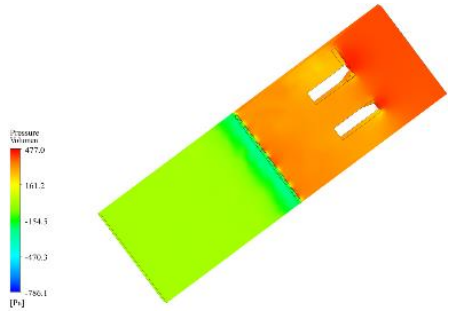

Figure 9: Pressure drop between the inlet and outlet of the control volume of the filter box

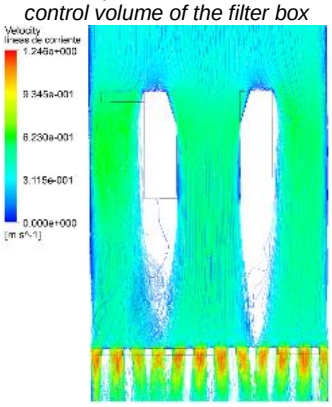

Figure 10: Current lines in cross section of the filter box

Figure 11 shows drop pressure in each perforation in a plane transverse of the filter box, this occurs because the crossbeams generate uneven flow entering the filter plate. The computational simulation of each speed required approximately 10 hours of computational calculations, in order for the solution to converge. Which in total translates into 100 hours of computational use to obtain the results.

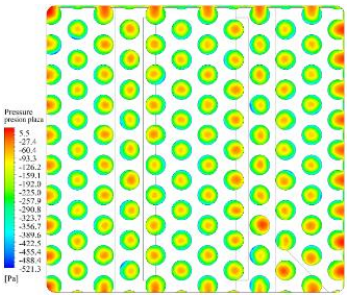

Figure 11: Plane transverse to the filter box shows the filter plate that a contour diagram is generated with the pressure

3.3.2.2 Simulation of the body; In Figure 12 the pressure drop occurs gradually, as is expected to occur in fluid flowing in parallel plates. In Figure 13 it can be seen that in the areas where the greatest drop pressure occurs are the entrance and exit of the body, due to the changes of geometries of the subsets. For the computational simulation of each velocity, approximately 15 hours of computational calculations were required for the solution to converge. Which in total translates into 150 hours of computational use to obtain the results.

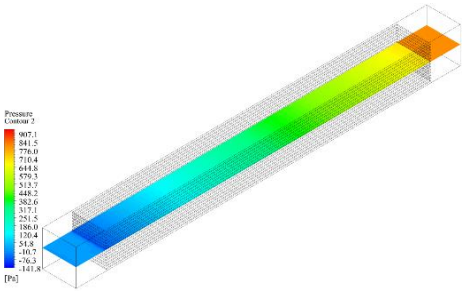

Figure 12: Pressure drop across a cooling channel

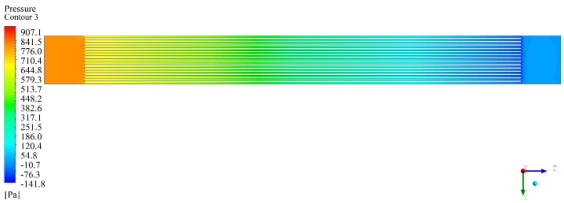

Figure 13: plane transverse to the channels through which the refrigerant circulates.

3.3.2.3 In the study of the nozzle, the drop pressure between the inlet and outlet of the nozzle control volume is shown in figure 14. Contour diagram is shown in a plane, which is at the center of the geometry, in which it can be seen that the highest drop pressure occurs in the top of the nozzle.

In figure 15 shows currents lines, where is observed that there is recirculation of the fluid in the zone of change of geometry;

Figure 16, there is a contour diagram in a plane which is in the transition from geometry (square to circular), where the recirculation of the refrigerant is corroborated.

For the computational simulation of each velocity, it took approximately 6 hours of computational calculations, in order for the solution to converge.

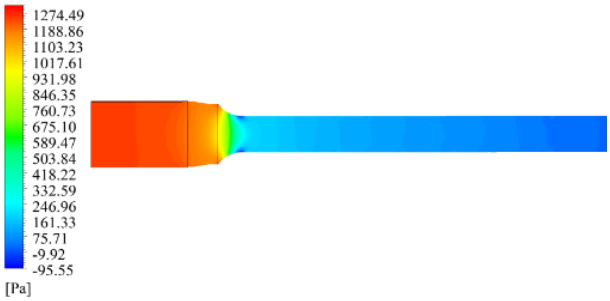

Figure 14: Pressure drop between the inlet and outlet of the nozzle control volume

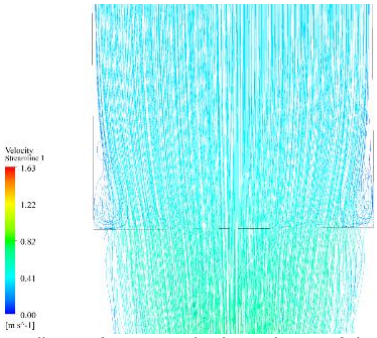

Figure 15: lines of currents in the volume of the nozzle. Recirculation occurs in the change of geometry.

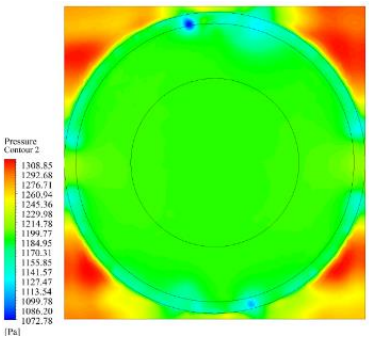

Figure 16: Transversal plane of the nozzle.

<u>3.3.2.4 Simulation of the Fuel Element</u>;
Figures 17, 18, 19 show results of the pressure drop for nominal speed in the fuel assembly. In Fig. 17 there is a volumetric diagram showing the distribution of the pressure drop in the complete volume. The filter plate, the entrance of the fuel plates and the throttling of the nozzle are the ones that generate the biggest difference. In figure 18 there is a plane through a channel of the refrigerant, where the gradual pressure drop in the parallel plates and the pressure drop in the nozzle are appreciated. Figure 19 shows a plane that is arranged transversally to the cooling channels, in this one can see how they affect the crossbeams in the low pressure.

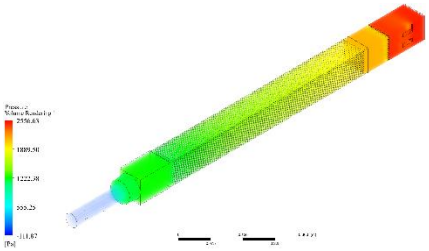

Figure 17: Distribution of the pressure drop between the input and output of the Fuel Element control volume.

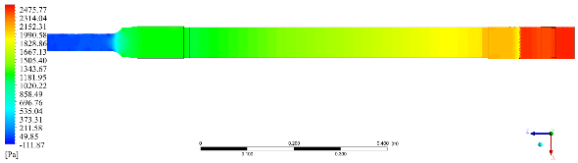

Figure 18: Plane showing the pressure drop between the input and output of the Fuel Element control volume.

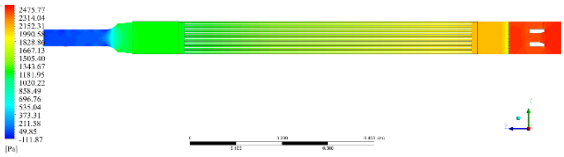

Figure 19: Plane transverse to the cooling channels of the control volume of the Fuel Element.

In figure 20, 21, 22, 23 the fuel assembly is characterized by current lines. In figure 20 the current lines are obstructed by the crossbeams, the orientation piece and filter plate. Figure 21 shows a stagnation of the water in the cooling channels. Then, Figure 22 shows the output of the current lines of the cooling channels, which produces an expansion, contributing in the pressure drop. And finally, Figure 23 shows an abrupt change of geometry in the nozzle, generating a pressure drop.

For the computational simulation of each speed, approximately 100 hours of computational calculations were required for the solution to converge. Which in total translates into 1000 hours of computational use to obtain the results.

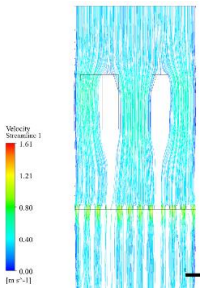

Figure 20

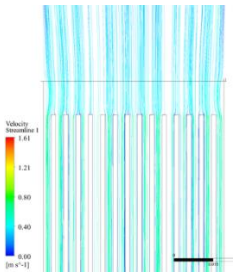

Figure 21

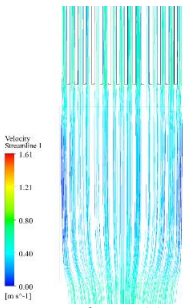

Figure 22

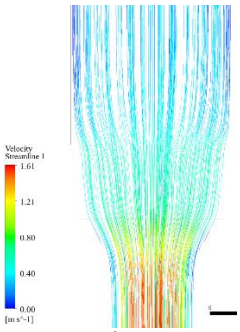

Figure 23

Figures 20, 21, 22 and 23 show results of the pressure drop for nominal speed in the fuel element.

4. Conclusions

The pressure drop results obtained by the analytical calculations are quite satisfactory, since they reach an order of magnitude very similar to the values of the nominal pressure losses. However, for the nominal speed (0,349 [m / s]) the result differs by 12.336 [Pa], which translates into a difference of 84%. For the velocity 1,15 [m / s] the pressure loss presents a variation of 13%.

The computational characteristics used greatly limit the use of tools, especially in the mesh. The 16 GB of RAM was not sufficient to incorporate the use of hexahedral elements to the walls and only allowed the use of tetrahedral elements. The use of the 4 cores also limited the computational capacity of the equations that solve the problem. The use of a computer of greater capacities would improve the mesh and would reduce the simulation time, which amounts to 1,290 hours.

The pressure contour diagrams and current lines determine the influence of each part on the pressure drop. The pieces that most influence are: the filter plate, the nozzle, the orientation piece and the crossbars.

It means all the zones where change of geometry happens and they can alter the route of the lines of current.

The subset method ensured the convergence of the mesh generated. Different techniques were applied effectively, simulating the behavior of the fluid in the nozzle in a satisfactory manner, however the high geometric complexity did not allow to replicate the methods in the other sub-assemblies nor in the complete fuel element.

The fuel body subset is the one with the greatest number of finite elements due to its larger size. The Filter Box, is the subset that has the greatest difficulty of meshing, due to the different parts that compose it. In the meshing of the fuel assembly is obtained an unstructured mesh composed of hexahedral elements, reaching 10 million finite elements. The four meshed volumes were validated using the Skewness method and Aspect Ratio method, being rated as very good to excellent and well below the limit.

5. References

[1] IAEA, «Good Practice for Qualification of High Density Low Enriched Uranium Research Reactor Fuel» INTERNATIONAL ATOMIC ENERGY AGENCY, Vienna, 2009.

[2] J. Daie, J. Medel, H. Torres, D. Calderón, L. Iturrieta y M. Loncomilla, «Descripción del Reactor RECH-1,» CCHEN, Santiago, 2004.

[3] D. Muñoz, «Diseño de un Loop Hidráulico Para Caracterización de Elementos Combustibles Nucleraes RECH-1,» Universidad de Chile, Santiago, 2016.

[4] Y. Bayazit, «Fluid mechanic phenomena relating to flow control in conduits and pumps,» University of Minnesota, Minnesota, 2014.

[5] I. Shame, Mecánica de Fluidos, Bogota, Colombia: McGraw-Hill, 1995.

[6] A. Valencia y R. Paredes, «Laminar flow and heat transfer in confined channel flow past square bars arranged side by side,» Heat and Mass Transfer, vol. 39, pp. 721-728, 2003.

[7] M. Versteeg, An Introduction to Computation Fluid Dynamics: THE FINITE VOLUME METHOD, Edinbugh Gate, Harlow, England: Person Education, 2007.

[8] Ansys Inc, ANSYS FLUENT User's Guide, Pennsylvania: Ansys inc, 2011.